

Making a Robust Interfacial Scaffold: Bijel Rheology and its Link to Processability

Matthew N. Lee, Job H. J. Thijssen, Jessica A. Witt, Paul S. Clegg, and Ali Mohraz*

Confocal microscopy and rheology studies of two bijel systems are presented to elucidate relationships between the physicochemical properties of bijels and their ability to be utilized as soft matter templates for materials synthesis. For the first time, the origins of viscoelasticity in these systems are investigated using conventional rheometry and a direct correspondence between the elastic storage modulus, particle loading, and the departure from criticality is observed. Further, the rheological transitions that accompany fluid re-mixing in bijels are characterized, providing key insights into the synergistic role of interfacial tension and interparticle interactions in mediating their mechanical robustness. Bijels that are predominantly stabilized by interfacial tension are also highly sensitive to gradients in chemical composition and more easily prone to mechanical failure during processing. Despite this increased sensitivity, a modified strategy for processing these more delicate systems is developed and its efficacy is demonstrated by synthesizing a bicontinuous macroporous hydrogel scaffold.

in a broad array of modern applications for their large and tunable interfacial area,^[4–6] efficient transport characteristics,^[7–9] enhanced structural integrity,^[10] and percolation of material properties.^[11,12] In two earlier papers, Lee and Mohraz showed how bijels could be employed as soft templates to synthesize a novel family of composites and hierarchically porous solids with tunable chemistry and co-continuous morphology at the nano- to micrometer length scales.^[13,14] These unique morphologies can radically transform the design paradigm for a number of functional composite materials including battery, fuel cell, and supercapacitor electrodes; catalyst supports; and tissue engineering scaffolds. Bijels have also been envisioned as efficient microfluidic cross-flow chambers for chemical reactions or separation processes, or as vehicles for controlled release.^[1,15,16]

1. Introduction

Bicontinuous interfacially jammed emulsion gels, or bijels, are an emerging class of non-equilibrium soft matter originally predicted by lattice-Boltzmann simulations and first realized experimentally in 2007.^[1,2] These materials are formed by arrested spinodal decomposition of partially-miscible fluid mixtures in the presence of colloidal particles with near-equal affinity for either fluid phase.^[3] Upon demixing, colloids initially dispersed in the single-phase fluid mixture sequester to the interface with typical desorption energies $\Delta G \sim 10^4 k_B T_{room}$ per particle, where k_B is Boltzmann's constant and T is the absolute temperature. The system then becomes jammed once the interfacial area is just sufficient to accommodate all the particles. The result is an intricate three-dimensional network of continuous fluid channels stabilized by a percolating particle monolayer. Materials with this unique bicontinuous morphology are valued

Given their novelty, elegance, complexity, unique and advantageous morphology, and the breadth of available outlets for their use, bijels show much promise as a new and emerging class of soft matter with a significant need for experimental studies that facilitate their proliferation in both research and industry. In this paper, we present a new set of confocal microscopy and rheology experiments that identify the key characteristics of bijels that mediate their processability into functional materials for the applications listed above.

The first bijels created in bulk consisted of critical mixtures of water and 2,6-lutidine (W/L) with a lower critical solution temperature (LCST) $\approx 34^\circ\text{C}$ and lutidine mole fraction $x_L = 0.064$, stabilized by colloidal silica particles.^[2] With this system, Lee and Mohraz subsequently developed reliable and flexible protocols for template-based synthesis of a variety of materials and composites with bicontinuous spinodal-like microstructure.^[13,14] Exposing a bijel to a liquid reservoir with selective miscibility in, or strong preference for, one of the fluid phases can alter the chemical composition inside the corresponding fluid channels. This allows the selective polymerization of fluid domains in a bijel (Figure 1), which is the key step for the processing protocol mentioned above. Here, the external reservoir consists of a liquid monomer that can be chemically crosslinked with exposure to ultraviolet light in the presence of a radical photoinitiator. The process provides control over a number of processing parameters given the abundance of hydrophobic/hydrophilic monomers that can be polymerized through free-radical reactions, the ability to control the polymer crosslink density, and wide control over the width of the fluid

M. N. Lee, J. A. Witt, Dr. A. Mohraz
Department of Chemical Engineering
& Materials Science
University of California
Irvine, CA 92697, USA
E-mail: mohraz@uci.edu

Dr. J. H. J. Thijssen, Dr. P. S. Clegg
SUPA, School of Physics and Astronomy
The University of Edinburgh
Mayfield Road, Edinburgh EH9 3JZ, UK



DOI: 10.1002/adfm.201201090

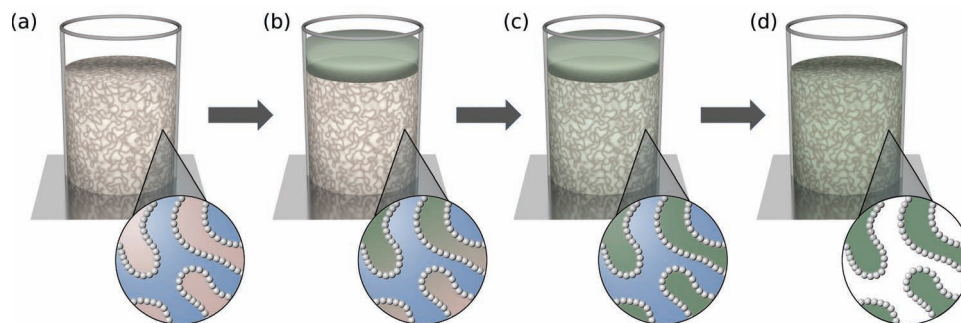


Figure 1. Schematic representation showing the selective polymerization of a bijel. a) A 3D bijel is formed by arrested spinodal decomposition of partially miscible fluids by colloidal particles that jam at the interface. b) The bijel surface is exposed to a reservoir of liquid monomer that preferentially partitions into one fluid phase. c) The fluid composition of one bijel phase is modified while preserving the morphology. d) The monomer is cured via UV photopolymerization to form a bicontinuous macroporous solid and the remaining liquid is drained.

channels (macropores in the polymerized scaffold) through the particle volume fraction and size.^[13,15] More recently, a new bijel system consisting of nitromethane and ethylene glycol (NM/EG) with an upper critical solution temperature (UCST) $\approx 40^\circ\text{C}$ and nitromethane mole fraction $x_{\text{NM}} = 0.633$, stabilized by silica microspheres was reported with several potential advantages over the W/L system.^[16] These included a more forgiving and reproducible method for tuning the particle-liquid affinities, a phase diagram with a higher degree of symmetry,^[17] and mechanical stability of the bijel (immiscibility of the fluid constituents) at room temperature. However, we observed that this system presented challenges for materials processing even with selectively miscible monomers; introduction of a monomer into this system typically resulted in mechanical failure and collapse of the bijel backbone. By exploring the rheological properties of these two bijel systems (W/L and NM/EG) we found that the extent of particle attraction at the interface mediates the bijel's ability to withstand changes in its chemical makeup without altering its morphology. Bijels stabilized by interfacial tension alone are more easily damaged or destroyed when subjected to steep gradients in chemical composition. This undesired breakdown could result from a spatially heterogeneous distribution of the interfacial tension and concomitant Marangoni stresses along the particle-laden interface,^[18] leading to deformation and rupturing of the fluid domains. Conversely, bijels formed with sufficiently attractive particles at the interface (e.g., via van der Waals forces^[19]) can offer enhanced stability against structural rearrangements during solvent exchange and provide a robust template for the synthesis of bicontinuous macroporous polymer scaffolds. Overall, our findings indicate that despite sharing a common genesis and morphology, the mechanical robustness and processability of bijels is strongly mediated by the details of interparticle interactions along the jammed interface, which will be of great significance to the practical use of bijels for advanced materials synthesis. More broadly, in any application of solid-stabilized emulsions involving compositional variations in the liquid phase such as Pickering drug delivery systems, the interfacial tension gradients induced by the payload may cause significant problems for emulsion stability and function. Here we address these issues in the context

of bijel processing, but our findings can also be directly applied to the broader class of Pickering systems that involve similar modes of interparticle interactions and interfacial phenomena.

2. Results and Discussion

For critical mixtures of W/L and NM/EG prepared with colloid volume fraction $\phi_p = 0.04$, the storage (G') and loss (G'') moduli are monitored over time as the suspensions are quenched from the single-fluid phase to different depths into the two-phase region (Figure 2a,b). The samples show rheological signatures of gelation, with a crossover point where G' becomes consistently larger than G'' after the phase boundary is crossed (Figure 2c). In both systems, we observe an increase in the terminal values of G' and G'' with deeper quenches, which likely follows from the increase in γ and a stronger adsorption of particles at the interface at greater departures from T_c .^[20] Here the values of γ approximately coincide for W/L samples ramped to $T = 60^\circ\text{C}$ ($T - T_c \approx 25^\circ\text{C}$) and NM/EG samples quenched to $T = 25^\circ\text{C}$ ($T_c - T \approx 15^\circ\text{C}$),^[20] (Supporting Information). However, the elastic modulus was larger for the W/L system by about an order of magnitude. We also note a more prominent aging behavior, as defined by a gradual but continuous growth in the elastic modulus, in the first 15 min after quenching the W/L samples, which slows down considerably by the 30-min mark. We attribute this behavior to gradual bonding of neighbor particles in a primary van der Waals minimum of the interparticle potential, and will return to this point later on in the paper. In NM/EG bijels the aging effects were less apparent and G' did not change significantly once the set temperature had been reached. We therefore used the NM/EG system in another experiment where both the departure temperature, $(T_c - T)$, and particle volume fraction, ϕ_p , were systematically varied to further investigate the origins and hallmarks of viscoelasticity in these systems. It has been theorized that elastic storage in bijels should scale as $G' \sim \gamma/L_D$, where L_D is the average width of the fluid domains, determined by the particle loading as $L_D \sim \phi_p^{-1}$.^[15] In addition, for binary fluids close to the critical point, the general relationship $\gamma(T) \sim (T_c - T)^\mu$ has been previously proposed, where

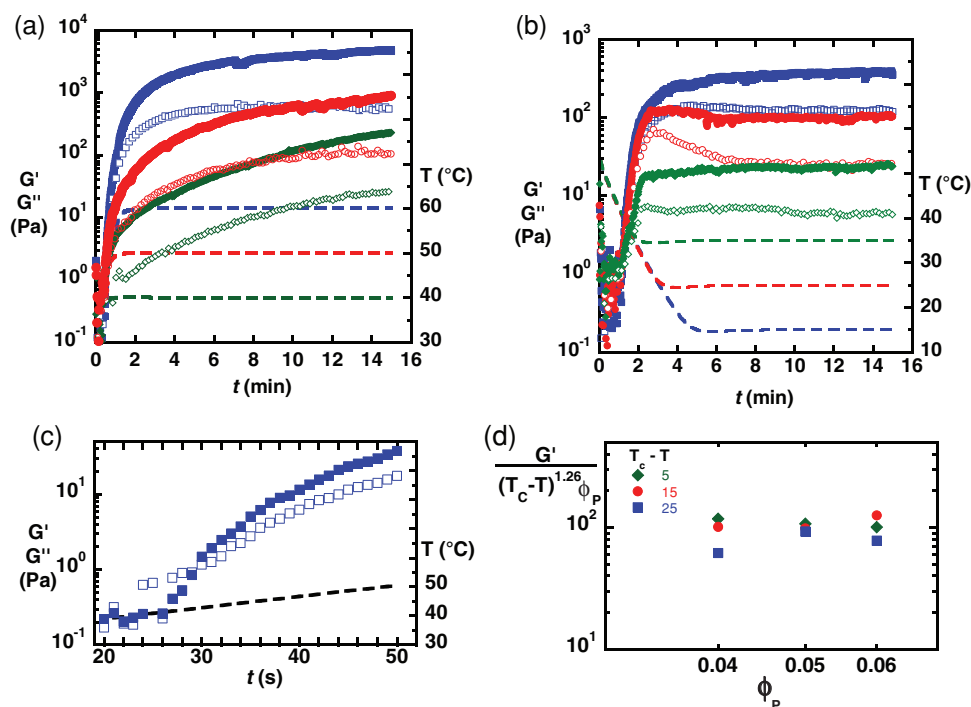


Figure 2. Evolution of G' (solid symbols) and G'' (open symbols) in critical mixtures of a) water/2,6-lutidine (W/L) and b) nitromethane/ethylene glycol (NM/EG) quenched to various temperatures. c) Crossover of G' and G'' as the phase boundary is crossed in the W/L system. d) Scaling of elastic storage with interfacial tension $\gamma(T)$ and ϕ_p in the NM/EG system.

$\mu = 1.26$ is the standard critical exponent.^[21,22] Experimentally we find that values of G' , when scaled by the product $\phi_p(T_c - T)^\mu$ are more or less constant with no obvious dependence on either ϕ_p or T (Figure 2d). Our finding supports the idea that stronger bijels may be formed with either 1) an increase in the concentration of stabilizing particles or 2) deeper temperature quenches. It also provides a means for simple quantitative comparison between different systems.

As mentioned earlier, our initial attempts to selectively polymerize NM/EG bijels following the protocol established for the W/L system were unsuccessful; introduction of a monomer typically resulted in mechanical failure of the bijel. Further, the situation was not improved by processing at lower temperatures ($T_c - T = 55$ °C) or using samples with higher solids content ($\phi_p = 0.08$). These observations suggest that processability of a bijel is not necessarily directly correlated to the primary determinants of its mechanical integrity, γ and L_D . Inspired by the qualitative differences between the evolutions of G' in Figure 2a,b, we asked whether a secondary effect such as particle interactions at the interface could play a role. W/L bijels are known to exhibit a fascinating transition in the first minutes after formation, where short-range van der Waals attraction between particles coupled with long-range electrostatic repulsion between charged surface groups induce particle bonding at the interface after an initial annealing period.^[19] The resultant bijel variant is known as a “monogel”, and here the particles are no longer held in place by interfacial tension alone and remain assembled as a percolating monolayer even when the fluids are re-mixed. This transition could potentially explain the more prominent aging behavior of

the W/L bijels in Figure 2a. We used confocal microscopy to visualize bijels as their fluid constituents were re-mixed, after a 20-min aging period in the jammed state (see Supporting Information videos SV1 and SV2). For the NM/EG system, the structure disintegrates upon raising the temperature above T_c and the scaffold is re-dispersed as primary particles and/or small clusters in the single fluid phase (Figure 3a). Even for aging periods over 24 h, the particles did not remain assembled at the interface after removing the interfacial tension (data not shown). In contrast, the jammed particle monolayer in W/L bijels remains intact with little or no change to the morphology as the liquid/liquid interface is removed (Figure 3b). In this series the image contrast is visibly reduced over time as the fluids re-mix and the refractive index mismatch between the fluid domains is removed.

To quantify these observations, we repeated the above experiments on the rheometer and monitored the storage and loss moduli as the fluids were re-mixed after a 20-min aging period. As expected, the NM/EG bijel loses its gel-like character upon transitioning to the single-phase region, with G' and G'' both falling below the instrument's sensitivity limit (Figure 4a). For the W/L system, the moduli both drop significantly after the interfacial tension is removed; however, gel-like character ($G' > G''$) is retained (Figure 4b), which is consistent with the monogel transition observed in Figure 3b. Further, when the monogel is subsequently broken by shearing at $\dot{\gamma} = 800$ s⁻¹, the particles do not re-aggregate and a liquid-like suspension is instead formed. This result underlines the essential role played by the temporary particle scaffold during monogel formation, which was predicted at the time of its initial discovery

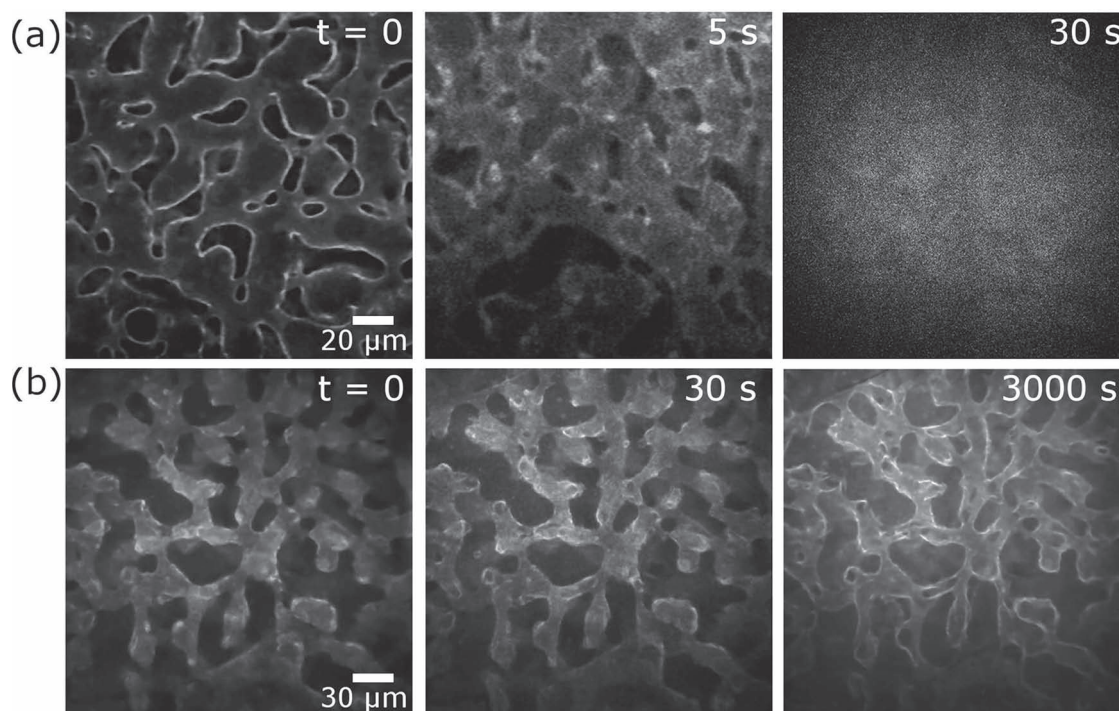


Figure 3. Time series of fluorescence confocal microscopy images showing the behavior of a) NM/EG bijels and b) W/L bijels as the liquids remix (i.e., the interfacial tension is removed).

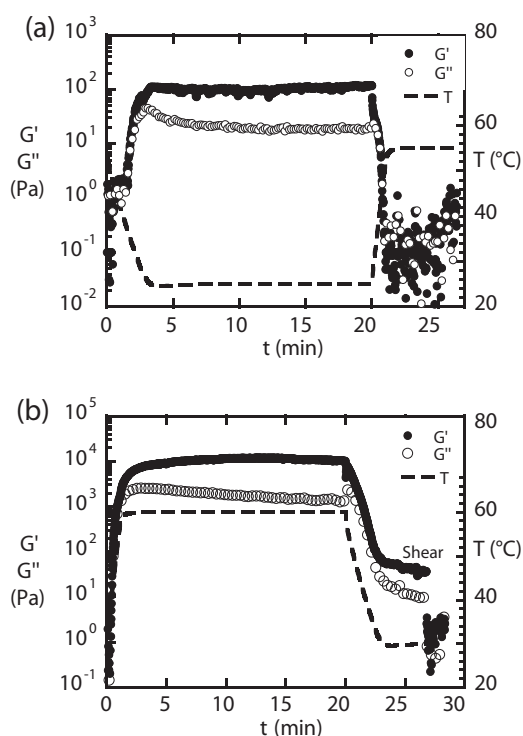


Figure 4. Rheological transitions observed in bijels of a) NM/EG and b) W/L as the liquids remix (i.e., the interfacial tension is removed).

but not observed until now.^[19] The behavior can be contrasted to conventional colloidal gels, which typically return to a gelled state after shearing ceases.

Collectively, the microscopy and rheology experiments shown in Figure 3 and 4 reveal markedly different behaviors in W/L and NM/EG bijels as the interfacial tension is removed, and we suspect that this distinction is highly relevant to bijel processing in the two systems. As mentioned earlier, the selective polymerization of W/L bijels is particularly robust; the system is compatible with 10 different monomers at present though this catalog is perpetually expanding (for a current list please see the Supporting Information). We infer that this flexibility is associated with the possibility of a monogel transition in the W/L system, considering that any of these same monomers tend to destroy the microstructure in NM/EG bijels. To illustrate these differences, we processed bijels in both systems by exposing their surfaces to reservoirs containing pure trimethylolpropane triacrylate (TMPTA) and poly(ethylene glycol) diacrylate (PEGDA). In the W/L system, these monomers selectively partition into the lutidine-rich phase and the bijel is transformed into a bicontinuous macroporous solid while preserving the spinodal microstructure (Figure 5). By contrast, the NM/EG bijels gradually collapse by contact with either monomer, despite the fact that both selectively partition into the NM-rich phase and lead to an overall increase in the interfacial tension between the fluid phases (+11.7% for TMPTA, +4.3% for PEGDA at 9% v/v, 25 °C); hence bijel breakdown cannot simply be attributed to an increase in fluid miscibility or decrease in interfacial tension.

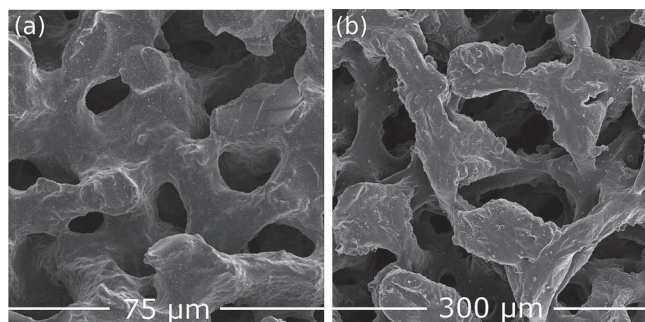


Figure 5. SEM images of W/L bijels selectively polymerized using a) pure TMPTA and b) pure PEGDA monomers.

We recognize that any significant perturbation of the local fluid composition can induce this undesired transition in the NM/EG system, even with the introduction of simple solvents like water or toluene. A possible explanation for this behavior is that the addition of a third component to the bijel microstructure results in a gradient of the liquid interfacial tension along the particle-laden interface and associated Marangoni stresses that can rupture the fluid domains in the absence of a sufficiently rigid particle network. Another possibility is that a substantial change in the fluid composition could alter the 3-phase contact angle of the particles sufficiently such that they detach from the interface. These issues appear to be inconsequential for processing of W/L bijels, where the particles supposedly become trapped in a primary energy minimum upon monogel formation and can conceivably resist structural rearrangements to a greater extent. For example, if the collapse of NM/EG bijels is due to a change in the contact angle, it is not surprising that a monogel-forming system can withstand this change. Similarly, bonding of particles in a primary minimum can provide resistance against tangential surface stresses and impart mechanical stability to the bijel backbone during solvent exchange. Therefore, we believe that the robustness of the W/L system for materials processing is fundamentally correlated to its ability for monogel formation.

All the same, the NM/EG mixture has several advantages over W/L and it is desirable to use this system for bijel processing. Drawing from our findings regarding the sensitivity of NM/EG bijels to steep gradients in composition, we are able to successfully polymerize this system using a reservoir of PEGDA diluted to 20% v/v with nitromethane (**Figure 6**).

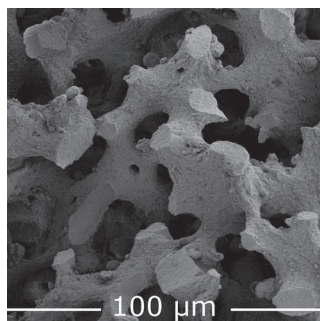


Figure 6. SEM image of an NM/EG bijel selectively polymerized using PEGDA monomer (20% v/v in nitromethane).

Using this strategy allowed the chemical composition of the fluid channels to be more gradually and subtly altered while preventing damage to the 3D spinodal microstructure. Similar to the W/L samples, the polymerized PEGDA scaffold retained the bicontinuous morphology of its bijel parent. These macroporous hydrogels could be valuable in cell and tissue engineering applications where biocompatible scaffolds with large, continuous pores are often desired to improve cell motility and transport of nutrients throughout the microstructure.^[23,24] Our attempts to substantially increase the PEGDA concentration in the reservoir or to use TMPTA in any amount necessary for sufficient crosslinking both led to the destruction of the bijel, which again highlights the sensitivity of this system to steep gradients in the chemical composition of either fluid phase. We note that while minimizing chemical gradients enables selective polymerization of NM/EG bijels, the process is significantly less flexible and reliable. Additionally, the time required for the monomer to traverse through the bijel microstructure is significantly longer (≈ 3 h for W/L bijels and 3 days for NM/EG bijels of the same volume and domain size). Nevertheless, our findings demonstrate that monogel formation is not strictly necessary for bijel processing, since we were able to successfully polymerize a NM/EG scaffold (**Figure 6**), which does not form a monogel (**Figure 3a**). Though in this paper we have focused on processing bijels through selective polymerization, the results presented here may have important consequences for any application where foreign components are introduced into bijels, for example in the controlled cross-flow of fluids for chemical reaction or extraction purposes.^[15] Overall it appears that particle attraction at the interface can strongly influence bijel rheology and functionality, and the ability to tune these interactions will be invaluable as other applications are developed for these soft materials.

A remaining question is why the monogel transition readily occurs in W/L but not in NM/EG systems. Previous studies have ascribed monogel formation to the bonding of particles in a primary van der Waals minimum.^[19] In the W/L system, attractive capillary forces and interfacial jamming drive the particles across a relatively weak electrostatic energy barrier into their primary van der Waals minimum, resulting in particle bonding^[25] and hence a robust monogel. In this system, the repulsive barrier only stems from the dissociation of unreacted silanol groups, endowing the particles with a weak, negative electrostatic charge. Considering the similarities in material properties (interfacial tension, dielectric constants, particle core chemistry) between the two systems, it is reasonable to assume that the same modes of attraction operate in the NM/EG system (i.e., van der Waals, capillary, and interfacial jamming), with comparable magnitudes. The different colloid surface chemistries used for the two binary fluid systems must then, directly or indirectly, give rise to the changes in bonding behavior. We hypothesize that the particles experience a larger repulsive barrier in the NM/EG system, impeding their bonding in a primary van der Waals minimum and thereby inhibiting monogel formation. This larger barrier may originate from solvation of the HMDS graft layer by deprotonated nitromethane molecules, which also contributes negative electrostatic charges to the particles. Based on the observed fragility of the interfacial scaffold in the NM/EG system, the combined dissociation/solvation

barrier succeeds in keeping the particles apart, thereby preventing a monogel transition in the NM/EG bijel.

3. Conclusions

In summary, we have used rheology and microscopy studies to investigate the origins of viscoelasticity in bijels and identify key factors that influence their functionality as soft templates for advanced materials synthesis. We observed that both particle loading and the departure from criticality govern the elastic storage modulus in bijels, and that robust bijel processing is presumably linked to attractive interactions between particles at the interface. In the absence of monogel formation, the particle-stabilized interface is more easily disrupted with the incorporation of foreign fluid species, leading to breakdown of the microstructure. Despite this increased sensitivity, we have extended our processing capabilities to the NM/EG system and synthesized bicontinuous, macroporous hydrogel scaffolds for potential use in cell and tissue engineering applications. Finally, our ability to study the rheology of these unique soft materials will enable future research on the fundamental properties of bijels and the influence of particle interactions on their flow properties.

4. Experimental Section

In common with previous bijel studies, here we used Stöber silica particles. However, in principle, a range of other particles chemistries such as metal oxides (titania, zirconia, or alumina) or polymers (poly(methyl methacrylate) or polystyrene) could be employed as long as their wettability could be controlled to the same degree as that of silica.

Particle Synthesis: Two types of fluorescent Stöber silica colloids with an average diameter of $\langle d \rangle = 410$ nm and a coefficient of variation $CV = 3.2\%$ were used in this study (Supporting Information). First, 12.5 mg of rhodamine B isothiocyanate dye (RITC, Sigma-Aldrich) was mixed with 50 mg of 3-aminopropyltriethoxysilane (APS, $\geq 98\%$, Sigma-Aldrich) in 10 mL of anhydrous ethanol and stirred for at least 12 hr. Particles were then synthesized by combining 35 mL of anhydrous ethanol, 10 mL ammonia solution (35% w/w, Fisher) and 5 mL of the conjugated dye solution in a flask, followed by the addition of 4.18 mL of tetraethylorthosilicate (TEOS, $\geq 99\%$, Sigma-Aldrich), subsequently stirring for at least 12 h.^[26,27] For NM/EG bijels, the surface chemistry of the particles was rendered partially hydrophobic by adding 3.5 mL of hexamethyldisilazane (HMDS, 98%, Alfa Aesar) directly to the reaction flask 3 h after the addition of TEOS. Particles used for the W/L system were not subject to this surface silanization step, but instead washed by repeated centrifugation in deionized water and carefully dried at 70 °C to achieve near-neutral wetting properties.^[25,28] For the NM/EG system, particles were washed in ethanol and dried at 120 °C under vacuum.

Formation and Processing of Bijels: W/L bijels were formed by dispersing the silica particles in ultrapure water using a sonic probe (Branson Sonifier 250). An appropriate amount of 2,6-lutidine was then added to give a near-critical composition (lutidine mole fraction $x_L \approx 0.064$), and 200, 300, or 600 μL of the single-phase suspension was transferred to cylindrical microscopy vials of 5, 7, or 15 mm inner diameter (i.d.), respectively. W/L bijels are formed upon warming ($LCST \approx 34$ °C), and these were prepared by ramping the samples into the unstable region in a microwave oven and quickly transferring them to an incubator maintained at 60 °C as described previously.^[13] NM/EG bijels form upon cooling ($UCST \approx 40$ °C), and were prepared by

dispersing the HMDS-modified silica in the critical mixture ($x_{NM} \approx 0.633$) via sonication, which concurrently heated the mixture above the UCST. The suspension was then transferred into thin capillaries preheated to 50 °C (400 μm path length, Vitrocom) and rapidly quenched into the unstable region by placing the containers on a chilled aluminum block. Bulk NM/EG bijels for materials processing were prepared in pre-heated cylindrical vials of 3 mm i.d. and quenched in an ethanol bath maintained at -10 °C.

Bijels were transformed into bicontinuous macroporous solids by selective polymerization of liquid UV-curable monomers as shown schematically in Figure 1. For this study trimethylolpropane triacrylate (TMPTA) and poly(ethylene glycol) diacrylate (M_w 600, PEGDA) that were kindly provided by Sartomer were used. The monomers were mixed with a photoinitiator (Darocur 1173, Ciba) and a reservoir was then placed on the top surface of a bijel to initiate the selective partitioning of the monomer solution into one fluid phase (Figure 1b). After complete solvent exchange (Figure 1c), the monomer-rich phase of the bijel was crosslinked using a UV lamp (Omnicure 1000), and the remaining liquid was drained (Figure 1d).

Microscopy: Bijels were imaged using a confocal scanner (Vt-eye, Visitech International) attached to an inverted microscope (Axio Observer, Carl Zeiss Microimaging, Inc.) with a 20 \times , NA = 0.4 objective. To assess the effect of fluid remixing on the microstructure, W/L bijels aged for 20 min in an oven at 60 °C were cooled to 20 °C on the microscope stage by free convection while the microstructure was visualized over time. An analogous experiment was performed with NM/EG bijels, instead using a steel block at 55 °C to warm specimens back into the single-phase region. Scanning electron microscopy (SEM) was performed on polymerized bijels using a Quanta 3D microscope (FEI Company). Prior to imaging, the silica particles were carefully etched from the polymer surfaces using an HF solution (10% v/v) and the samples were dried thoroughly before depositing a thin layer of iridium onto their surfaces using a sputter coater (South Bay Technologies).

Rheology: Rheological measurements were performed using a stress-controlled rheometer (MCR 301, Anton-Paar) with parallel-plate geometry and a gap height of 100 μm . Bijels were formed on the rheometer stage using an integrated Peltier heating/cooling system operating at the maximum available rates of about 25 and 10 °C/min for heating and cooling, respectively. The rheometer was also equipped with a Peltier hood to promote a uniform temperature throughout the sample, and minimize solvent evaporation. For each sample, critical suspensions initially in the single-fluid phase were transferred onto the rheometer stage maintained at either 30 °C (W/L) or 55 °C (NM/EG) and pre-sheared at $\dot{\gamma} = 800$ s $^{-1}$ for 30 s. Samples were then quenched into the two-phase region while recording the storage and loss moduli (G' and G'' , respectively) every 1 s at a constant oscillatory strain of $\gamma = 0.1\%$ and frequency $f = 1$ Hz to monitor the gelation process. In some experiments the samples were allowed to age for a given duration and then heated or cooled back into the single-phase region. The measurements were found to be reproducible and geometry-independent, indicating that our results were not contaminated by wall slip (Supporting Information).

Interfacial Tension Measurements: Nitromethane (99+%, Acros Organics), ethylene glycol (99.8%, Sigma Aldrich) and toluene (Fisher Scientific) were used as received. The monomer TMPTA (Sartomer, SR351) or PEGDA (Sartomer, SR610) was mixed with photoinitiator 2-hydroxy-2-methylpropiophenone (Aldrich = Darocur 1173) at a mass ratio of 99:1. Such mixtures were pipetted into the NM-rich phase at volume ratios of $\approx 1:10$. Interfacial tensions were measured using the pendant-drop method on a Krüss EasyDrop instrument (model FM40Mk2), equipped with a level environmental chamber (Thermostat TC3010), connected to a circulator (Julabo F12). The temperature near the sample, ranging from 15.8 to 33.8 °C, was monitored with a thermocouple (LakeShore 331). The chamber was sealed with parafilm and regularly flushed with dry nitrogen gas to avoid contamination with (condensed) water. A rectangular glass container had been filled with the less dense phase (EG-rich), while a glass syringe (needle diameter

1.82 mm, Starrett micrometer) contained the droplet phase (NM-rich). Droplets were delivered at a set flow rate of 100 $\mu\text{L}/\text{min}$ to volumes of 9 to 28 μL using a computer-controlled dosing unit, and were allowed to equilibrate for ≈ 5 min before digital snapshots were recorded from the side. As the needle reservoir can be at a different temperature than the needle tip (which is in the environmental chamber), droplets had a tendency to shrink over time. Hence, results were regularly checked for their dependence on equilibration time (2.5 to 15 min) and droplet volume. Interfacial-tension values were extracted by fitting the Young-Laplace equation to the recorded drop profiles. Results are very sensitive to the densities provided for the liquid mixtures. Therefore, the liquid densities were measured at the corresponding temperatures using a density meter (Anton Paar, DMA 4500). Interfacial-tension errors are estimated to be 0.035 mN/m at room temperature up to 0.058 mN/m at lower/higher temperatures.

Supporting Information

Supporting Information is available from the Wiley Online Library or from the author.

Acknowledgements

M.N.L. and J.A.W. acknowledge the U. S. Department of Education for GAANN fellowships. J.H.J.T is currently funded through the Royal Society of Edinburgh/BP Trust Personal Research Fellowship. A.M. acknowledges UC Irvine for startup funds and a CORCL award.

Received: April 19, 2012

Revised: August 2, 2012

Published online: September 3, 2012

- [1] K. Stratford, R. Adhikari, I. Pagonabarraga, J. C. Desplat, M. E. Cates, *Science* **2005**, 309, 2198.
- [2] E. M. Herzig, K. A. White, A. B. Schofield, W. C. K. Poon, P. S. Clegg, *Nat. Mater.* **2007**, 6, 971.
- [3] P. S. Clegg, *J. Phys.-Condens. Mater.* **2008**, 20, 113101.
- [4] N. Ishizuka, H. Kobayashi, H. Minakuchi, K. Nakanishi, K. Hirao, K. Hosoya, T. Ikegami, N. Tanaka, *J. Chromatogr. A* **2002**, 960, 85.
- [5] Y. Ding, M. Chen, J. Erlebach, *J. Am. Chem. Soc.* **2004**, 126, 6876.
- [6] B. H. Jones, T. P. Lodge, *J. Am. Chem. Soc.* **2009**, 131, 1676.
- [7] H. Y. Chen, Y. Kwon, K. Thornton, *Scripta Mater.* **2009**, 61, 52.
- [8] S. Torquato, S. Hyun, A. Donev, *Phys. Rev. Lett.* **2002**, 89, 266601.
- [9] H. Zhang, X. Yu, P. V. Braun, *Nat. Nanotechnol.* **2011**, 6, 277.
- [10] L. Wang, J. Lau, E. L. Thomas, M. C. Boyce, *Adv. Mater.* **2011**, 13, 1524.
- [11] B. Soares, F. Gubbels, R. Jérôme, P. Teyssié, E. Vanlathem, R. Deltour, *Polym. Bull.* **1995**, 35, 223.
- [12] F. Gubbels, R. Jérôme, E. Vanlathem, R. Deltour, S. Blacher, F. Brouers, *Chem. Mater.* **1998**, 10, 1227.
- [13] M. N. Lee, A. Mohraz, *Adv. Mater.* **2010**, 22, 4836.
- [14] M. N. Lee, A. Mohraz, *J. Am. Chem. Soc.* **2011**, 18, 6945.
- [15] M. E. Cates, P. S. Clegg, *Soft Matter* **2008**, 4, 2132.
- [16] J. W. Tavacoli, J. H. J. Thijssen, A. B. Schofield, P. S. Clegg, *Adv. Funct. Mater.* **2011**, 21, 2020.
- [17] J. Sørensen, W. Arlt, *Liquid-liquid equilibrium data collection*, Vol. 1, Dechema, Frankfurt **1979**.
- [18] S. Berg, *Phys. Fluids* **2009**, 21, 032105.
- [19] E. Sanz, K. A. White, P. S. Clegg, M. E. Cates, *Phys. Rev. Lett.* **2009**, 103, 255502.
- [20] C. A. Grattoni, R. A. Dawe, C. Y. Seah, J. D. Gray, *J. Chem. Eng. Data* **1993**, 38, 516.
- [21] B. Widom, *J. Chem. Phys.* **1965**, 43, 3892.
- [22] J. S. Rowlinson, B. Widom, in *Molecular Theory of Capillarity*, Dover Publications, Mineola, NY **2002**.
- [23] M. Martina, G. Subramanyam, J. C. Weaver, D. W. Huttmacher, D. E. Morse, S. Valiyaveetil, *Biomaterials* **2005**, 26, 5609.
- [24] S. G. Lévesque, R. M. Lim, M. S. Shoichet, *Biomaterials* **2005**, 26, 7436.
- [25] K. A. White, A. B. Schofield, B. P. Binks, P. S. Clegg, *J. Phys.-Condens. Mater.* **2008**, 20, 494223.
- [26] A. van Blaaderen, A. Vrij, *Langmuir* **1992**, 8, 2921.
- [27] G. Bogush, M. Tracy, C. Zukoski IV, *J. Non-Cryst. Solids* **1988**, 104, 95.
- [28] K. A. White, A. B. Schofield, P. Wormald, J. W. Tavacoli, B. P. Binks, P. S. Clegg, *J. Colloid Interface Sci.* **2011**, 1, 126.